



Adsorption performance of modified graphene oxide nanoparticles for the removal of toluene, ethylbenzene, and xylenes from aqueous solution

Avideh Azizi^a, Ali Torabian^{b,*}, Elham Moniri^c, Amir Hessam Hassani^a, Homayon Ahmad Panahi^d

^aDepartment of Environmental Engineering, Science and Research Branch, Islamic Azad University, Poonak sq. Ashrafi Esfahani Blv., Hesarak, Tehran 14515-775, Iran, emails: avideh_85@yahoo.com (A. Azizi), ahhassani@srbiau.ac.ir (A.H. Hassani)

^bFaculty of Environment, University of Tehran, No. 25, Ghods St., Enghelab Ave., Tehran 14155-6135, Iran, Tel. +0098 91 2125 7996; Fax: +0098 21 6640 7719; email: atorabi@ut.ac.ir

^cDepartment of Chemistry, Varamin (Pishva) Branch, Islamic Azad University, Shahrak Naghsh Jahan, Pishva 33817-74895, Iran, email: moniri30003000@yahoo.com

^dDepartment of Chemistry, Central Tehran Branch, Islamic Azad University, Shahrak Ghods, Simaye Iran, Tehran 14676-86831, Iran, email: h.ahmadpanahi@iauctb.ac.ir

Received 21 January 2016; Accepted 20 May 2016

ABSTRACT

The purpose of this study was to investigate the effect of graphene oxide nanoparticles modified with 4-aminodiphenylamine (GO-A) on the removal of toluene, ethylbenzene, and p-,o-xylene (TEX). Nano-sorbent was characterized using Fourier transform infrared resonance spectroscopy, carbon, hydrogen and nitrogen elemental analysis, Brunauer-Emmett-Teller analysis, and transmission electron microscopy. The effect of different experimental parameters including contact time, pH, and initial concentration of adsorbate and adsorbent were examined. According to the results, an optimum TEX removal efficiency was observed at contact time = 5 min, pH 4, and adsorbent dose = 1 g/L at 20 mg/L initial TEX concentration. Besides, the point of zero charge (pH_{pzc}) was evaluated to be 4. The adsorption isotherms (Langmuir, Freundlich, and Dubinin–Radushkevich) and kinetics (pseudo-first-order, pseudo-second-order, intraparticle diffusion, and Elovich) were used to indicate the isotherm and kinetic parameters. The adsorption process followed Langmuir isotherm and pseudo-second-order kinetic. Finally, GO-A was regenerated at seven cycles for the TEX removal confirming its good regeneration capacity.

Keywords: Graphene oxide; Adsorption; TEX; Nano-adsorbent; Regeneration

1. Introduction

Nowadays, many industrial activities produce various types of anionic, cationic, and organic pollutants [1]. These contaminants are discharged into water resources and environment. Therefore, contami-

nation of resources by organic compounds has become an important environmental problem in recent years. The hazardous aromatic hydrocarbons exist in the effluent of industrials such as petroleum industry producing gasoline and diesel fuel [2,3]. These compounds can be contaminated water resources via leakage of petrol from the storage tanks [4]. Toluene,

*Corresponding author.

ethylbenzene, and xylenes are the persistent and toxicity compounds which are found in most of the contaminated sites [4]. Toluene and xylenes are also used as solvent in other industries polluting soil, air, groundwater, and surface water [5,6]. The maximum permissible concentration of toluene, ethylbenzene, and xylenes in drinking water are 0.7, 0.3, and 0.5 mg/L, respectively [7]. These compounds have irreparable impression in human health including: cancer, respiratory problems, and disruption of liver and kidney, irritation of mucosal membranes and hematological changes [2,3]. Therefore, it is necessary to remove these compounds from the environment.

Several methods are available for the removal of oil pollutants from aqueous environment such as: in situ burning, mechanical collection, chemical dispersants, bioremediation, and adsorption [8]. Adsorption is the one of the best techniques used for the removal of contaminants from water resources and wastewater [9]. Adsorption has been suggested as an excellent treatment method due to the features such as simple design, easy to adapt, economical, low production of toxic byproducts, and high efficiency [10–12]. Among the adsorbents, carbon base materials have special properties such as structural diversity, low density, chemical stability, and suitability for large-scale production. These features have aroused a lot of attraction in research in the last few decades [10].

Graphene is the one of the new-developed material from carbon groups and an allotrope of carbon [13,14]. The structure of graphene is composed of one single-thick sheet and two dimensional layers of sp^2 carbon atoms [15]. Graphene-based material has many beneficial properties such as: large specific surface area, high electron mobility at room temperature, stable electronic, and mechanical properties, high thermal conductivity, specific magnetism [13,14]. Due to these graphene-specific properties, it has been increasingly used as an effective adsorbent [16]. One derivative of graphene is graphene oxide (GO) that is used widely [17]. GO sheets consist of functional groups such as: carboxyl, hydroxyl and carbonyl groups [18]. Furthermore, GO is the graphene functionalized with groups of oxygen [19]. GO has some advantages compared to other adsorbents due to its low cost and environmentally friendly nature [8]. In addition, chemical modification of graphene and GO can increase its applications [10,20]. On the other hand, researchers have found out that graphene can be reused for at least five times without decreasing its adsorption efficiency [10]. Therefore, reusing of the residual material of the adsorption process for several times has an economic value [21].

In this study, GO was synthesized and modified with 4-aminodiphenylamine. Afterwards, adsorption of toluene, ethylbenzene, and p-,o-xylene (TEX) from aqueous solution using GO-A was investigated. For this purpose, the effects of contact time, pH, adsorbent dose, and initial TEX concentration on the performance of adsorption process were studied. Isotherm and kinetic adsorption studies were also conducted for planning of adsorption systems and determination of adsorption mechanism, respectively. Finally, the regeneration test were performed on the adsorbents (GO and GO-A) for several cycles and the results were compared.

2. Experimental section

2.1. Materials

All of the materials in this study were purchased from Merck, except for petroleum ether which was obtained from Romil pure chemistry. The characteristics of the materials are as follows: Graphite powder ($<50\ \mu\text{m}$, $\geq 99.5\%$), H_2SO_4 (95–97%), NaNO_3 , KMnO_4 , H_2O_2 (30%), HCl (37%), cyanuric chloride ($\geq 99\%$), 4-aminodiphenylamine ($\geq 98\%$), sodium chloride, methanol (purity $\geq 99.5\%$), sodium acetate trihydrate, acid acetic (100%), sodium hydrogen phosphate, sodium dihydrogen phosphate, toluene (purity $\geq 99\%$), ethylbenzene (purity $\geq 99\%$) and xylene (purity $\geq 99.8\%$). Physico-chemical properties of TEX are shown in Table 1.

2.2. Preparation of GO

GO was synthesized from graphite powder using the method introduced by Hummers and Offeman [23]. At first, 230 ml of the concentrated H_2SO_4 was added to the 5 L beaker containing a mixture of graphite (10 g) and NaNO_3 (5 g). The mixture was stirred for 1 h at room temperature. Then, 30 g of KMnO_4 were gradually added into the mixture. The beaker was placed in ice water bath. After 2 h of stirring, 460 ml of distilled water was added to the beaker and this reaction created a small amount of gas. Afterwards, 325 ml of H_2O_2 (30%) was added to the solution slowly in order to reduce the surplus KMnO_4 . Suspension was bubbling while stirring for 2 h. During the reaction, the temperature kept between 90 and 100°C . As soon as the color of suspension became greenish yellow, the mixture was filtered by filter paper. The cake was washed using HCl (3%) and the suspension was stirred for 1 h to remove the sulfite ions. Finally, the filter cake was washed by distilled water for several times until pH reached to the neutral

Table 1
The physicochemical properties of TEX [2,3,22]

Property	Toluene	Ethylbenzene	Xylenes
Formula	C ₆ H ₅ CH ₃	C ₆ H ₅ CH ₂ CH ₃	C ₆ H ₄ (CH ₃) ₂
Density (g/ml)	0.867	0.867	0.868
Polarity	Non-polar	Non-polar	Non-polar
Solubility at 20°C	515	152	150–198 ^a
Molar weight (g/mol)	92.15	106.18	106.18
Boiling point (°C)	111	136	137–144 ^a

^aDepends on type of xylene (m-, p-, and o-xylene).

level of seven. The GO was dried at 45°C for 2 d in oven and finally characterized by Fourier transform-infrared resonance (FTIR) (Thermo Nicolet, model: NEXUS 870 FT-IR, USA), carbon, hydrogen, and nitrogen (CHN) (Eager 300 for 1112, USA) and Brunauer–Emmett–Teller (BET) (BELSORP-mini II, Japan) techniques.

2.3. Coupling of GO with cyanuric chloride

Cyanuric chloride was prepared using the procedure proposed by Heydarinasab et al. [24]. About 1 g of GO was added into an Erlenmeyer flask. Then, 40 ml of petroleum ether was added. Erlenmeyer flask was sealed with plastic stopper and the mixture was stirred for 1 h at 350 rpm. The suspension was dispersed in distilled water by ultrasonic bath (Ultrasonic cleaner, model: WUC-A03H, Korea) for 30 min. Afterwards, 1 g of cyanuric chloride was added to the mixture and placed on a rotary shaker (IKA, KS 260 Basic, Korea) for 10 h at 100 rpm. The solution was remained for only 24 h. Suspension was then washed with 25 ml of petroleum ether and stirred for 24 h. Finally, the mixture was filtered and dried. The coupling of GO with cyanuric chloride (GO-C) was characterized by FTIR spectroscopy.

2.4. Modification of GO-C

At first 4-aminodiphenylamine (0.5 g) was added to a boiling flask. The mixture of acetate sodium buffer solution (pH 5, 0.01 M) and methanol were added to the flask. This solution was stirred at room temperature until 4-aminodiphenylamine was fully dissolved. The GO-C was added to the mixture and the suspension was shaken at 70–80°C for 2 d. After filtering, sediment was washed sequentially with the solution of sodium chloride, acetate sodium buffer, distilled water, and methanol. Finally, the sediment was filtered and dried for 2 d at 35–40°C temperature. GO-A

was characterized by FTIR, CHN, BET, and transmission electron microscopy (TEM) (model: EM 208, PHILIPS Co., Czech Republic) techniques.

2.5. Preparation of the TEX stock solutions

A 50 mg/L TEX stock solution was prepared in volumetric flask (with methanol solution). Using a micropipette, 29 µl of each mono aromatic was added to a 500 ml volumetric flask filled with distilled water. Then, the solution was placed in an ultrasonic bath and the mixture was shaken at room temperature. The stock solution was diluted by distilled water to reach to the desired concentration. The Standard solutions of TEX were prepared at the concentrations of 0.5, 1, 5, 10, 20, and 50 mg/L as follows: to prepare 50 ml of 0.5 mg/L solution, 0.5 ml of the 50 mg/L stock was added into a 50 ml volumetric flask filled with distilled water. This procedure was repeated for 1, 5, 10, 20 mg/L by adding 1, 5, 10, 20 ml of stock solution into a 50 ml flask, respectively.

2.6. Chemical analysis method

The TEX concentrations in water were determined using gas chromatography equipped with flame ionization detector. The samples were injected directly into the GC-FID system. The conditions of GC-FID (Agilent GC, 6890N) used for the measurement of TEX were as follows:

Sampling method: head space.

Detector: FID (heater: 250°C and makeup: 45 ml/min and air, flow: 350 ml/min and H₂ flow: 40 ml/min).

Injection technique: split (2:1), injector temperature: 210°C, injection volume: 2 µl.

Carrier gas: N₂, flow rate: 1.7 ml/min.

Column used: type of column: capillary, length: 30 m, diameter: 0.32 mm, film thickness: 0.25 µm, phase: HP-5.

Temperature program: initial temperature: 40°C, isothermal: 3.5 min, rate: 3°C/min, to: 65°C.

Isothermal: 0 min, rate: 30°C/min, to: 220°C, isothermal: 1 min.

2.7. Batch adsorption experiments

Batch adsorption tests were carried out to investigate the effects of the following parameters: contact time (1, 2, 3, 4, 5, 8, 60, 120, and 180 min), initial pH (4, 5, 6, 7, and 8), initial adsorbate concentration (0.3, 1, 7, 15, 20, 30, and 75 mg/L) and adsorbent dose (0.02, 0.1, 0.2, 0.6, 1, 2, and 4 g/L) for the removal of TEX from aqueous solutions using GO-A at room temperature. Solutions of TEX with adsorbent were placed in 100 ml of boiling flask and were covered with parafilm. Afterwards, suspensions were placed on a rotary shaker (150 rpm). The mixture was filtered with syringe filter (with 0.22 µm pore size). Finally, the concentrations of the clear supernatant were determined using absorbance values measured before and after the adsorption by GC-FID. The amount of TEX adsorption was calculated according to these equations:

$$q_t = \frac{(C_0 - C_t)v}{m} \quad (1)$$

$$\text{RE}(\%) = \left(\frac{C_0 - C_t}{C_0} \right) 100 \quad (2)$$

2.8. Determination of point of zero charge (pH pzc)

The point of zero charge of the nano-adsorbent was determined between at the pH range of 3 and 8 using sodium acetate–acetic acid buffer solutions and buffer of sodium hydrogen phosphate–sodium dihydrogen phosphate. 25 ml of each solution with pH varying from 3 to 8 was put in a 250 ml flask. Then, 0.05 g of the adsorbent was added into the flasks. These flasks were placed on rotary shaker for 24 h at 150 rpm. The final pH of the solutions was measured by pH meter (CRISON, Basic 20, Spain). Graph of ΔpH (final pH minus initial pH) was plotted against the initial pH and the point where ΔpH = 0 is selected as the point of zero charge (PZC).

2.9. Mathematical models for batch experiments

2.9.1. Isotherm mathematical models

Adsorption isotherms were calculated considering Langmuir, Freundlich, and Dubinin–Radushkevich models.

The Langmuir isotherm describes homogeneous adsorption systems and this model is reasonable for monolayer adsorption with negligible interaction between the sorbate molecules [25,26]. The linearized Langmuir isotherm is shown in (Eq. (3)) [27,28]:

$$\frac{C_e}{q_e} = \frac{1}{k_1 Q_m} + \frac{C_e}{Q_m} \quad (3)$$

The constants of Langmuir (k_1 and Q_m) can be obtained from the intercept and slope of the plot of C_e/q_e against C_e .

Freundlich isotherm model is nonlinear with the following assumptions: heterogeneous surfaces, limited sorption sites and variable potential energy interactions. Linear formulation of this model is expressed as follows [29,30]:

$$\log q_e = \log k_f + \frac{1}{n} \log C_e \quad (4)$$

where k_f and n can be determined from the intercept and slope of the linear plot of $\log q_e$ vs. $\log C_e$ respectively.

The expression of the Dubinin–Radushkevich isotherm is given by Eq. (5) [2,27]:

$$\ln q_e = \ln q_m - B\varepsilon^2 \quad (5)$$

In which, ε is polanyi potential, which is described as:

$$\varepsilon = RT \left(1 + \frac{1}{C_e} \right) \quad (6)$$

where E (the adsorption energy) is investigated for mechanism of adsorption reaction and is shown in the equation below:

$$E = \frac{1}{\sqrt{2B}} \quad (7)$$

The physical and chemical adsorption mechanisms accrue in the range of $E < 8$ kJ/mol and $E > 16$ kJ/mol, respectively. In the case of $8 < E < 16$ kJ/mol, it is identified as ion exchange mechanism [2].

2.9.2. Kinetic mathematical models

Four models were used to interpret the kinetic batch experimental data: pseudo-first-order, pseudo-second-order, intraparticle diffusion, and Elovich model.

The pseudo-first-order equation is expressed as follows [31,32]:

$$\log(q_e - q_t) = \log q_e - \frac{k_1}{2.303} t \quad (8)$$

The values of constants (k_1 and q_e) can be obtained from the slope and intercept of the linear plot of $\log(q_e - q_t)$ vs. t .

Pseudo-second-order model is represented by (Eq. (9)) [27,28,31]:

$$\frac{t}{q_t} = \frac{1}{q_e^2 k_2} + \frac{t}{q_e} \quad (9)$$

The plot of t/q_t vs. t gives k_2 and q_e values.

The intraparticle diffusion model equation can be formulated as follows [2]:

$$q_t = k_p t^{0.5} + c \quad (10)$$

In which, k_p is the slope of the plot of q_t vs. $t^{0.5}$.

The simple Elovich model equation can be expressed as [27]:

$$q_t = a - b \ln t \quad (11)$$

The values of constants a and b can be obtained by plotting q_t against $\ln(t)$.

2.10. Error functions

In the isotherm and kinetic studies, error analysis was used to evaluate the fit of the model to the experimental equilibrium data. The correlation coefficient (R^2) and qui-quadrado (Chi-square, χ^2) were calculated in this study. The error function is the sum of squares of the differences between experimental and calculated data in models with each squared difference divided by the corresponding calculated value. The equation is shown in (Eq. (12)) [33,34]:

$$\chi^2 = \sum_{i=1}^p \left(\frac{(q_e - q_{cal})^2}{q_e} \right) \quad (12)$$

The best isotherm and kinetic model were selected considering the minimum error function value.

2.11. The regeneration

The regeneration of the adsorbent was carried out through the following procedure: the 5 min contact

time, pH of 4, initial TEX concentration of 20 mg/L, adsorbent dose of 1 g/L, temperature of 23°C and agitation speed of 150 rpm. The GO-A and GO were washed by methanol and distilled water and the adsorbents were used for several times. The supernatant was filtered with syringe filter (with 0.22 μm pore size) after centrifugation (5 min, 3,000 rpm). Finally, the samples were analyzed by GC-FID.

3. Results and discussion

3.1. Adsorbent characteristics

The synthesized adsorbents were characterized by FTIR, CHN, BET, and TEM.

FTIR spectra for GO, GO-C, and GO-A is shown by the Fig. 1.

The FTIR spectrum of GO confirms that the peaks observed at 1,054 and 1,222 cm^{-1} are due to the stretching vibration of C–O groups [18,35]. The band peak at 1,421 cm^{-1} is attributed to the CH_2 stretching [36]. The stretching vibration which appears at 1,720 cm^{-1} is assigned to the C=O groups [35,37]. The aliphatic C–H peak at 2,922 cm^{-1} is broadened [18,35]. The peaks at 1,628 and 3,440 cm^{-1} are highly likely due to the existence of the O–H group [38,39].

In the spectrum of GO-C, the peaks at 1,410 and 1,458 cm^{-1} are assigned the bond of C=N [35,40]. The adsorption peak at 3,084 cm^{-1} may be also ascribed to the aromatic C–H bonds [41]. The FTIR spectra of GO-A exhibits the bands at 1,492 and 1,578 cm^{-1} due to C=N bonds [35,40]. A band at 1,718 cm^{-1} appears due to the C=O stretching [37]. The band at 3,402 cm^{-1} is attributed to the O–H and N–H groups [39,42].

The amount of carbon, hydrogen, and nitrogen in the GO and GO-A were quantitatively determined by CHN elemental analysis. Chemical composition of samples is shown in Table 2. CHN elemental analysis revealed that the percentage of carbon and nitrogen are increased via the modification of GO with 4-aminodiphenylamine (from 54.69%, 0.15% to 63.07%, 2.83% for C and N). It may be due to functional groups which attach to the GO sheets. The model of modified GO is illustrated in Fig. 2.

The textural properties of the adsorbents were determined by N_2 adsorption/desorption isotherms at 77 K using a BELSORP instrument. BET analysis was used to measure the BET surface area of samples. The total pore volume and average pore diameter were calculated by the Barrett-Joyner-Halenda (BJH) method and the total pore volume was computed from the adsorbed amount at a relative pressure (P/P_0) of 0.990. The textural characteristics of the adsorbents are presented in Table 3. The specific

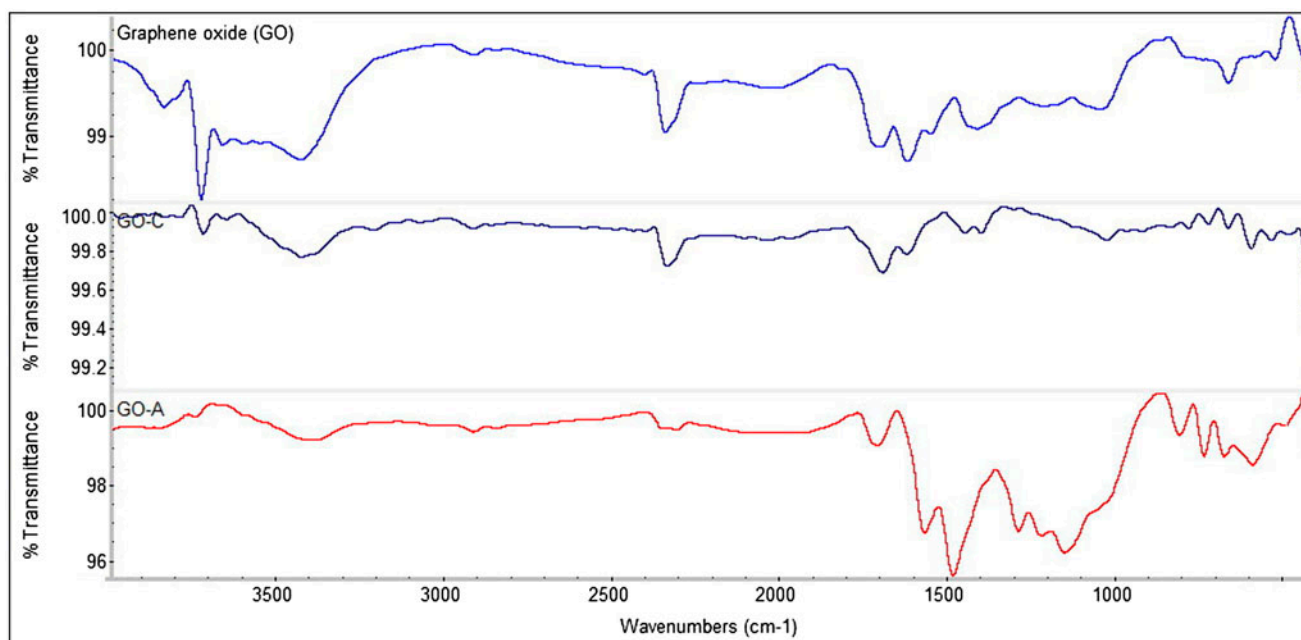


Fig. 1. FTIR spectra of GO, GO-C, GO-A.

Table 2
CHN analyses of GO and GO-A

Samples	C (%)	H (%)	N (%)
GO	54.69	2.46	0.15
GO-A	63.07	1.59	2.83

surface area of GO-A is $12.41 \text{ m}^2/\text{g}$, which is slightly lower than that of GO ($13.24 \text{ m}^2/\text{g}$). But the total pore volume and average pore diameter of GO-A ($0.133 \text{ cm}^3/\text{g}$, 42.879 nm) are much higher than that of GO ($0.016 \text{ cm}^3/\text{g}$, 4.853 nm). It can be explained by the fact that some groups connected to graphene layers act as spacers, resulting in the enhanced pore size distribution during aggregation [43].

Transmission electron microscope was used for samples at 100 kV. TEM analyze is applied for morphologic characterization of nanomaterials [13]. The TEM photos of GO-A are shown in Fig. 3. This photo illustrates that the sheets of GO-A consist of one to several layers (Fig. 3(a)). GO-A has some wrinkles and folds, indicating that the sheets have the flexibility of whole nanosheet (Fig. 3(b)). Thick and crumples are assigned to abundant oxygen-containing functional groups on the sheets [44]. These phenomena demonstrate that the GO-A paper is prepared properly. The length of nanosheets are also observed 100–300 nm (Fig. 3).

3.2. Adsorption performance

3.2.1. Effect of contact time

The behavior of TEX adsorption efficiency on GO-A was studied in wide range of 1–180 min. The concentration of TEX was quantified by GC-FID. The effect of contact time on TEX adsorption capacity (q_e) is displayed in Fig. 4. It can be seen that adsorption capacity of adsorbent was increased sharply in the first minutes (0–5 min). After, it decreased from 5 to 60 min. The adsorption capacity finally became constant from 60 to 180 min, approximately. The high-speed adsorption during the initial time is possibly due to available surface sites on the sorbent [45]. A similar result was reported by other researchers mentioning that the maximum adsorption occurred at the initial stage of time [13,45,46]. Therefore, the equilibrium time was selected as 5 min throughout this study. These findings could be confirmed that GO-A has very high adsorption capacity at the very beginning.

3.2.2. Effect of pH

In this step, the effect of solution pH (at the range of 4–8) was investigated. The solutions pH range of 4–5 were adjusted with sodium acetate-acetic acid buffer solutions and The solutions pH ranging from 6 to 8 were assessed with buffer of sodium hydrogen phosphate-sodium dihydrogen phosphate. The effects

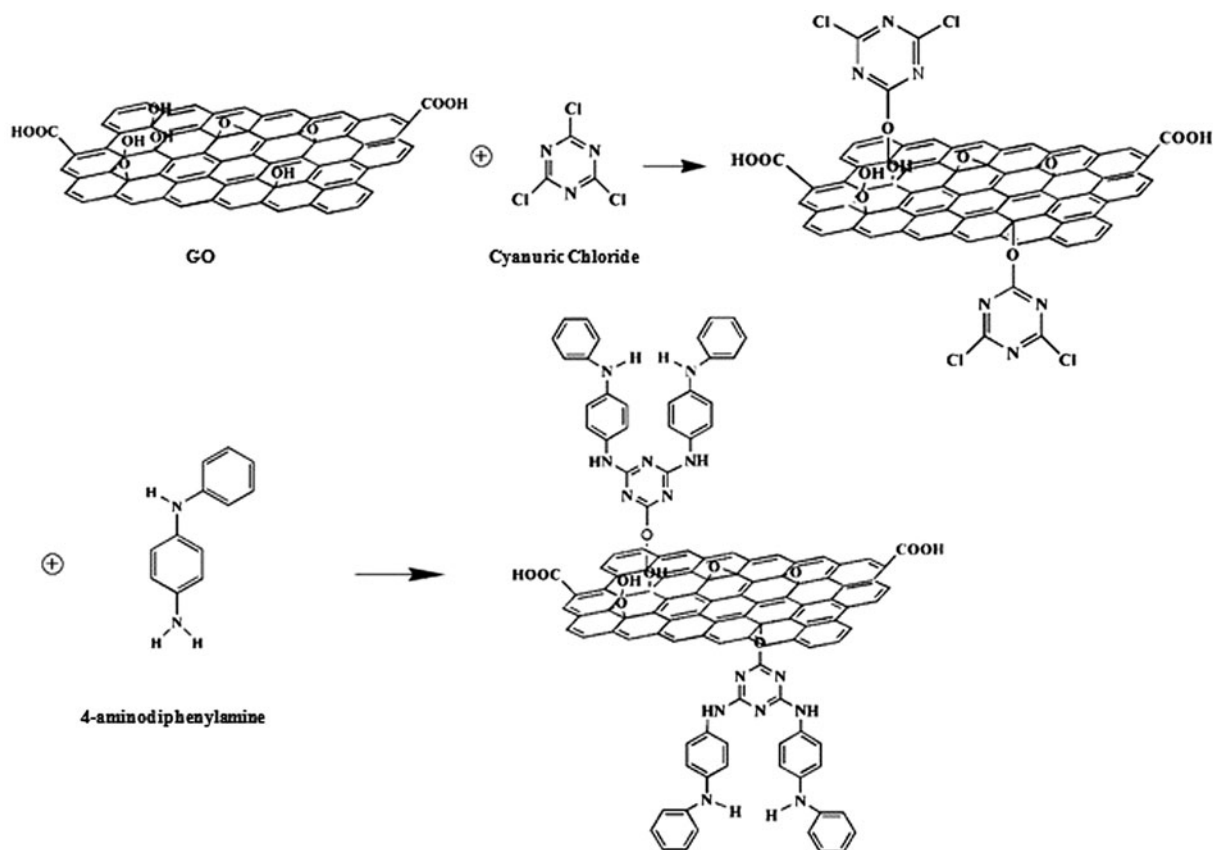


Fig. 2. Illustration of modified GO structure.

Table 3
Textural property of the GO and GO-A

Sample	BET surface area (m ² /g)	Total pore volume (cm ³ /g)	Average pore diameter (nm)
GO	13.24	0.016	4.853
GO-A	12.41	0.133	42.879

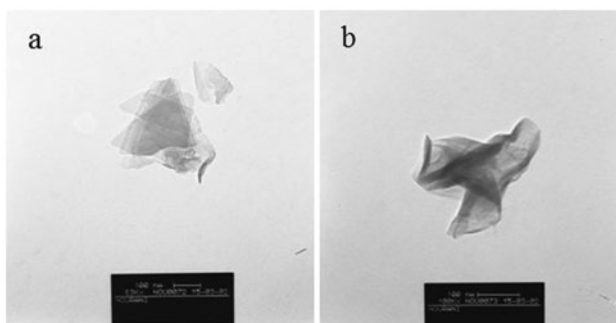


Fig. 3. The TEM images of GO-A (a and b, the scale bar is 100 nm).

of pH on adsorption capacity are shown in Fig. 5. The maximum adsorption capacity was observed at pH of 4. It can be deduced that the H⁺ ions in acetic acid establish interactions of hydrogen with adsorbent. As a result, the adsorbent transformed from hydrophilic to hydrophobic state increasing the removal efficiency at pH 4.

Moreover, the point of zero charge (pH_{PZC}) confirms the mechanism of the adsorption that surfaces of the adsorbent had zero net charge at this point (pH 4) [31].

The point of zero charge (PZC) for nano-adsorbent was determined in this study and the results revealed that the PZC was around pH 4. This finding can be

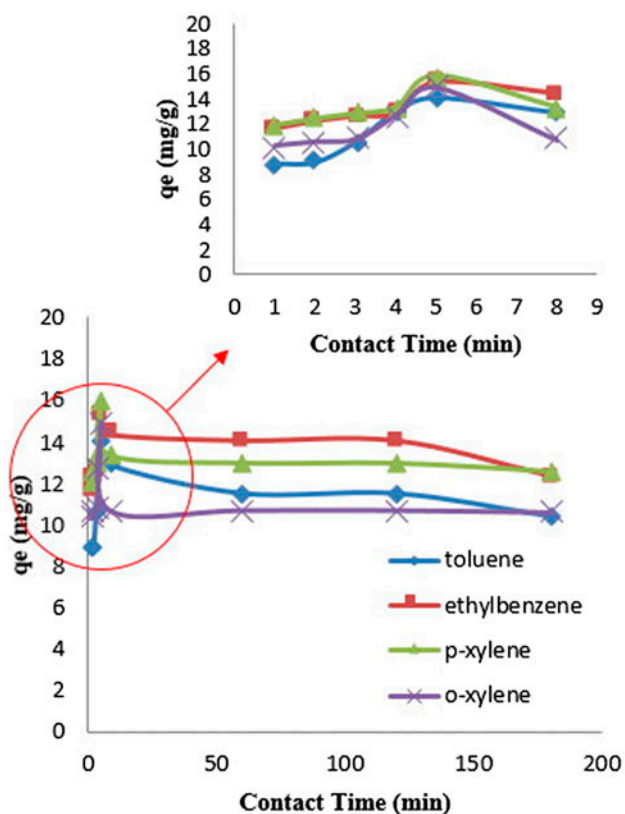


Fig. 4. The effect of contact time on TEX adsorption by GO-A (pH 4; initial concentration of TEX = 20 mg/L; adsorbent dose = 1 g/L; agitation speed = 150 rpm; room temperature = 23 °C).

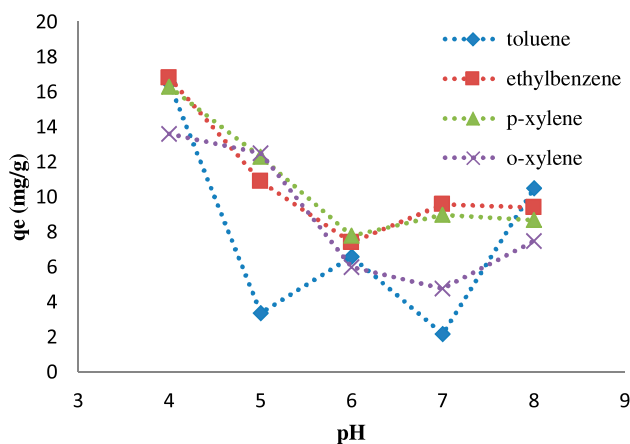


Fig. 5. The effect of pH on TEX adsorption by GO-A (contact time = 5 min; initial concentration of TEX = 20 mg/L; adsorbent dose = 1 g/L; agitation speed = 150 rpm; room temperature = 23 °C).

explained by the fact that the optimum adsorption of TEX occurred at pH 4 and thereafter adsorbent has no

more affinity. It may be due to the surface charge of adsorbent is positive and negative in $\text{pH} <$ and $>$ pH_{pzc} , respectively.

3.2.3. Effect of adsorbate concentration

Behavior of TEX adsorption capacity on nano-adsorbent was studied with changing the initial TEX concentrations under the range of 0.3 to 75 mg/L. This concentration range was chosen according to the range suggested by Seifi et al. [47]. Fig. 6 presents the effect of initial TEX concentration on adsorption capacity of the GO-A.

As seen in Fig. 6, adsorption capacity was increased with the increasing of TEX concentration. Similar results were reported by Nourmoradi et al. [2]. The finding of this study can be explained by the fact that the structure of TEX having the van der Waals force and moreover, driving force of TEX compounds increase on sites of adsorbent for adsorption at higher concentrations [2].

3.2.4. Effect of adsorbent dose

The experiments of this stage were performed at a wide range of adsorbent dose from 0.02 to 4 g/L. The ability of nano-adsorbent to adsorb TEX is shown in Fig. 7.

The removal efficiency of the four compounds was increased with increasing the adsorbent dose from 0.02 to 4 g/L. The removal efficiency was significantly low at the adsorbent dose of 0.02 g/L. Then, the removal efficiency increased to 46, 62, 64, and 58% for

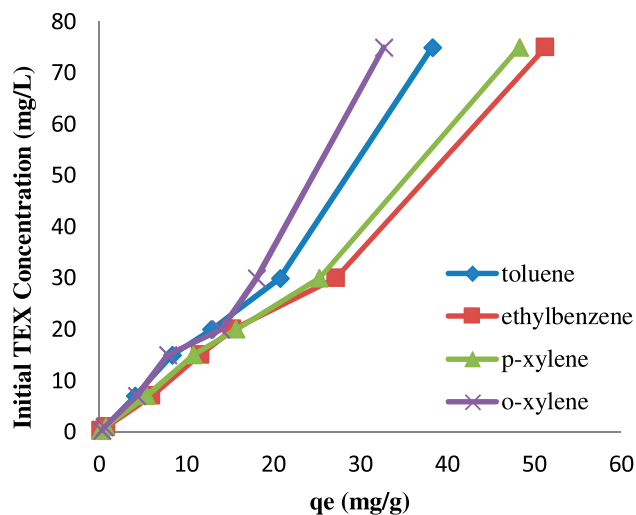


Fig. 6. The effect of initial TEX concentration on adsorption capacity of GO-A (contact time = 5 min; pH 4; adsorbent dose = 1 g/L; agitation speed = 150 rpm; room temperature = 23 °C).

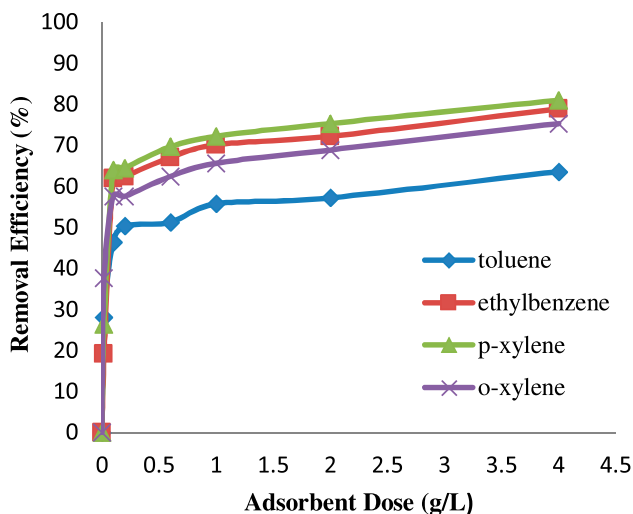


Fig. 7. The effect adsorbent dose (GO-A) on removal of TEX (contact time = 5 min; pH 4; initial concentration of TEX = 20 mg/L; agitation speed = 150 rpm; room temperature = 23 °C).

toluene, ethylbenzene, p-xylene (p-X), and o-xylene (o-X), at the adsorbent dose of 0.1 g/L, respectively. Removal efficiency of 56% (toluene), 70% (ethylbenzene), 72% (p-xylene), and 66% (o-xylene) were obtained at 1 g/L of adsorbent dose. It is noteworthy that after the dose of 1 g/L, the TEX removal efficiency was increased with a low rate. Therefore, the adsorbent dose of 1 g/L was considered as the optimum adsorbent concentration. The reason of TEX removal efficiency improvement with increasing the adsorbent dose is that the surface area of the adsorbent, the available sites for the adsorption process as well as the active functional groups increased with increasing the adsorbent concentration [27,34,45,48]. On the other hand, the adsorption capacity decreased due to the aggregation of particles decreasing the effective Surface area [45].

Fig. 7 also illustrates that the removal efficiency of the pollutants decreased in the order of p-xylene > ethylbenzene > o-xylene > toluene. The difference in the removal efficiency is attributed to four factors: (1) water solubility (p-X = 198 mg/L, $E = 152$ mg/L, o-X = 175 mg/L and $T = 515$ mg/L), (2) Molecular weight (p-X = 106 g mol^{-1} , $E = 106$ g mol^{-1} , o-X = 106 g mol^{-1} and $T = 92$ g mol^{-1}), (3) Hydrophobicity (based on their octanol–water coefficient log values) (p-X = 3.15, $E = 3.15$, o-X = 2.77 and $T = 2.69$) [2,3], and (4) Molecular size affecting the active surface sites available for the adsorption [46]. The results of this section were in agreement to those reported by other researchers for the same compounds [2,3].

3.2.5. Adsorption isotherms

The adsorption isotherm was studied considering the following conditions: contact time = 5 min, pH 4, initial concentration of TEX = 20 mg/L, agitation speed = 150 rpm, and the range of 0.1–4 g/L for the adsorbent dose. Three isotherm models (Langmuir, Freundlich and Dubinin–Radushkevich) were studied to analyze the mechanism of the adsorption process.

The Langmuir, Freundlich, and Dubinin–Radushkevich parameters as well as the correlation coefficient (R^2) are presented in Table 4. The correlation coefficient values of the models were compared. The R^2 values of the Langmuir model were higher than the linear correlation coefficient (R^2) from the other models. Langmuir correlation coefficient was evaluated to be 0.928, 0.961, 0.974, and 0.981 for toluene, ethylbenzene, p-xylene, and o-xylene, respectively (Fig. 8). The Langmuir constant (k_i) was negative proving that increasing the adsorbent dose does not have high impact on the adsorption. The E parameter in the Dubinin–Radushkevich isotherm is shown in Table 4. The E values of TEX adsorption were in the range of 0.296–0.5405 kJ/mol. Considering the results, the dominant mechanism was physical adsorption.

3.2.6. Kinetics of adsorption

The kinetic of TEX adsorption on nano-adsorbent was studied at the pH of 4, initial TEX concentration of 20 mg/L, adsorption dose of 1 g/L, agitation speed of 150 rpm, and a range of 1–5 min for contact time. Pseudo-first-order, pseudo-second-order, intraparticle diffusion, and Elovich models were studied.

Table 5 shows the kinetic models for the adsorption of TEX from aqueous solutions by nano-adsorbent. The results revealed that the adsorption process followed the pseudo-second-order model considering its relatively high values of the R^2 comparing to that of the other models. The R^2 values for pseudo-second-order model were 0.931, 0.963, 0.963, and 0.928 for toluene, ethylbenzene, p-xylene, and o-xylene, respectively (Fig. 9). The values of q_e (experimental) and q_e (calculated) of the pseudo-first-order and pseudo-second-order are presented in Table 5. The values of q_e (calculated) for pseudo-second-order model were near to the values of q_e (experimental). It was observed that the pseudo-second-order model accurately predicts the experimental results rather than the pseudo-first-order model.

Table 4
Adsorption isotherms constants

	Langmuir			Freundlich			Dubinin–Radushkevich		
	k_1 (L/mg)	Q_m (mg/g)	R^2	k_f (L/mg)	n	R^2	B (mol ² /kJ ²)	E (kJ/mol)	R^2
Toluene	-0.0932	1.5244	0.9281	4.6×10^{-8}	0.1131	0.8913	5.7135	0.2958	0.8567
Ethylbenzene	-0.1324	3.2383	0.9609	9.899×10^{-4}	0.1802	0.8892	2.0188	0.4977	0.8193
p-Xylene	-0.1402	3.7636	0.9742	3.1564×10^{-3}	0.1942	0.9135	1.7114	0.5405	0.8443
o-Xylene	-0.1233	2.7167	0.9809	3.0931×10^{-4}	0.1707	0.8891	2.4007	0.4563	0.8309

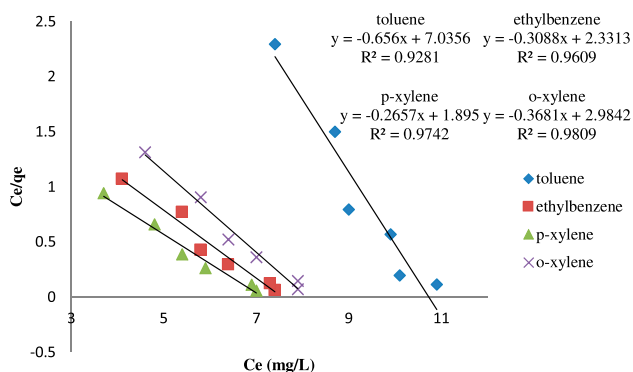


Fig. 8. Langmuir isotherm model for the TEX removal by GO-A.

3.2.7. Error analysis

The error functions were calculated for the isotherm and kinetic models. Table 6 lists the values of the correlation coefficient (R^2) and error function for TEX adsorption on GO-A. Langmuir model offered the most accurate prediction among all the models tested for toluene, ethylbenzene, p-xylene, and o-xylene. Moreover, pseudo-second-order model was observed as the best kinetic model.

3.2.8. Regeneration of adsorbents

Regeneration of GO-A was carried out by washing procedure (with methanol and distilled water) for seven cycles. The results are illustrated in Fig. 10.

Table 5
Adsorption kinetic constants

	Toluene	Ethylbenzene	p-Xylene	o-Xylene
$q_{e(\text{experimental})}$ (mg/g)	14.1	15.3	15.9	14.9
<i>Pseudo-first-order</i>				
k_1 (1/min)	0.5037	0.1315	0.1460	0.2262
$q_{e(\text{calculated})}$ (mg/g)	11.1969	4.1200	4.5477	6.4313
R^2	0.7922	0.9716	0.993	0.7295
<i>Pseudo-second-order</i>				
k_2 (g/mg min)	0.0382	0.1084	0.0963	0.0588
$q_{e(\text{calculated})}$ (mg/g)	17.54	15.8730	16.6389	16.5837
R^2	0.9309	0.963	0.9625	0.9284
<i>Intraparticle diffusion</i>				
k_p (mg/g min ^{1/2})	4.5442	2.4881	2.6964	3.4833
c	3.5019	8.7288	8.8196	6.0203
R^2	0.8848	0.7294	0.7444	0.7616
<i>Elovich model</i>				
a	7.9422	11.176	11.48	9.4778
b	3.3189	1.8008	1.9423	2.488
R^2	0.8049	0.6516	0.6587	0.6626

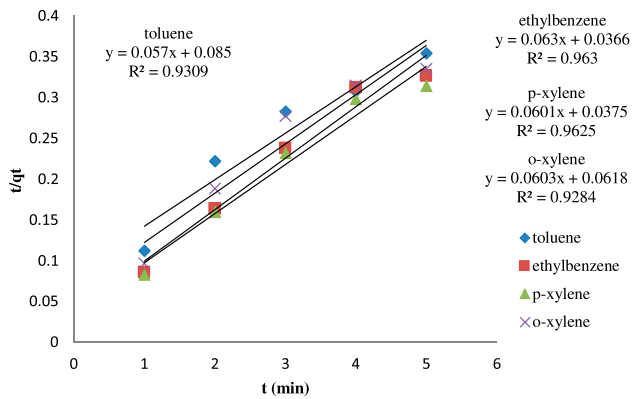


Fig. 9. Pseudo-second-order model for the TEX removal by GO-A.

The findings of the regeneration study showed that the removal efficiency increased at the first cycles (cycle number: 1 to 3) and afterwards, it became almost constant for the TEX compounds. Considering the obtained results, GO-A with at least seven cycles can be suggested as an efficient adsorbent without any

significant loss in its adsorption capacity. Similar results for regeneration of graphene family were observed by other researchers [10,13]. The regeneration test was also performed for GO (for four cycles) and the results were compared to the removal efficiency of GO-A (Fig. 11). As seen in Fig. 11, the removal efficiency of GO-A was higher than that of GO in all the regeneration cycles. The modification of GO should be the reason of the higher adsorption capacity of GO-A compared to GO. According to the obtained results (Table 3), this modification process helped to form the nano-adsorbent with larger pore volume and diameter than GO (about 10-fold). The larger pore volume increases the surface of the active sites improving the rate of the reactant diffusion [49]. Thus, pore volume has specific role in enhancing the adsorption capacity of graphene [44]. Another reason could be the functionalized groups and benzene rings in GO-A which are higher than GO affecting the π - π interaction resulting in the increasing of the adsorption capacity. Consequently, modification of adsorbent can be developed adsorption capacity [43].

Table 6
Error function of models for TEX adsorption onto GO-A

	Toluene	Ethylbenzene	p-Xylene	o-Xylene
<i>Langmuir</i>				
R^2	0.8850	0.7590	0.8118	0.8959
χ^2	15.0968	30.6630	47.1797	15.9545
<i>Freundlich</i>				
R^2	0.8316	0.7049	0.5467	0.6679
χ^2	22.8007	31.3689	58.1867	30.7551
<i>Dubinin–Radushkevich</i>				
R^2	0.7421	0.5760	0.4279	0.5654
χ^2	30.7138	48.3686	78.1797	42.5951
<i>Pseudo-first-order</i>				
R^2	0.4931	0.5701	0.6018	0.6734
χ^2	1.0445	0.6525	0.6096	0.8761
<i>Pseudo-second-order</i>				
R^2	0.8583	0.7858	0.8093	0.8180
χ^2	0.3827	0.2033	0.2185	0.3456
<i>Intraparticle diffusion</i>				
R^2	0.8848	0.7294	0.7444	0.7616
χ^2	0.2604	0.1584	0.1666	0.3047
<i>Elovich model</i>				
R^2	0.8048	0.6516	0.6586	0.6625
χ^2	0.4301	0.2016	0.2204	0.4232

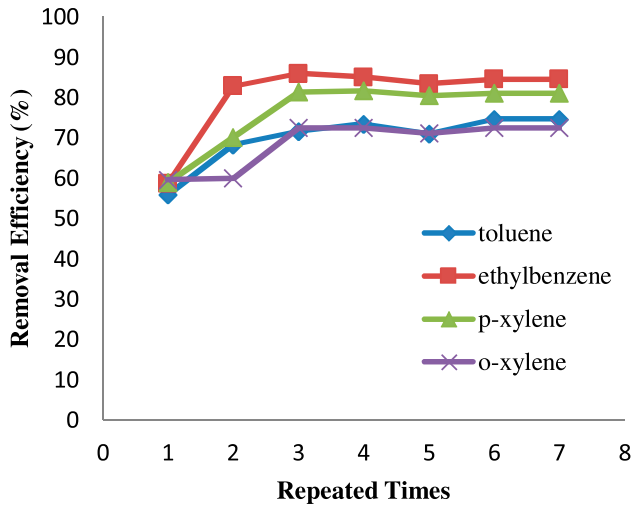


Fig. 10. The regeneration of GO-A (contact time = 5 min; pH 4; initial concentration of TEX = 20 mg/L; adsorbent dose = 1 g/L; agitation speed = 150 rpm; room temperature = 23°C).

3.2.9. Comparison of different adsorbents for TEX adsorption

Table 7 compares the q_e values obtained in this study with those of other adsorbents including zeolite, carbon nanotube, activated carbon, montmorillonite modified with poly ethylene glycol, smectite organoclay, thermally modified diatomite, and ostrich bone waste-loaded a cationic surfactant. It is observed that the GO-A studied in this research has a good adsorption capacity for TEX removal. This suggests that the GO-A is efficient for TEX adsorption. Besides, the GO-A had better performance in TEX removal at the beginning of the adsorption process than other adsorbents. This characteristic is desirable for the industrial applications, which need rapid adsorption process for emergency condition. Hence, the GO-A possesses of good capability for treatment of TEX-containing wastewaters.

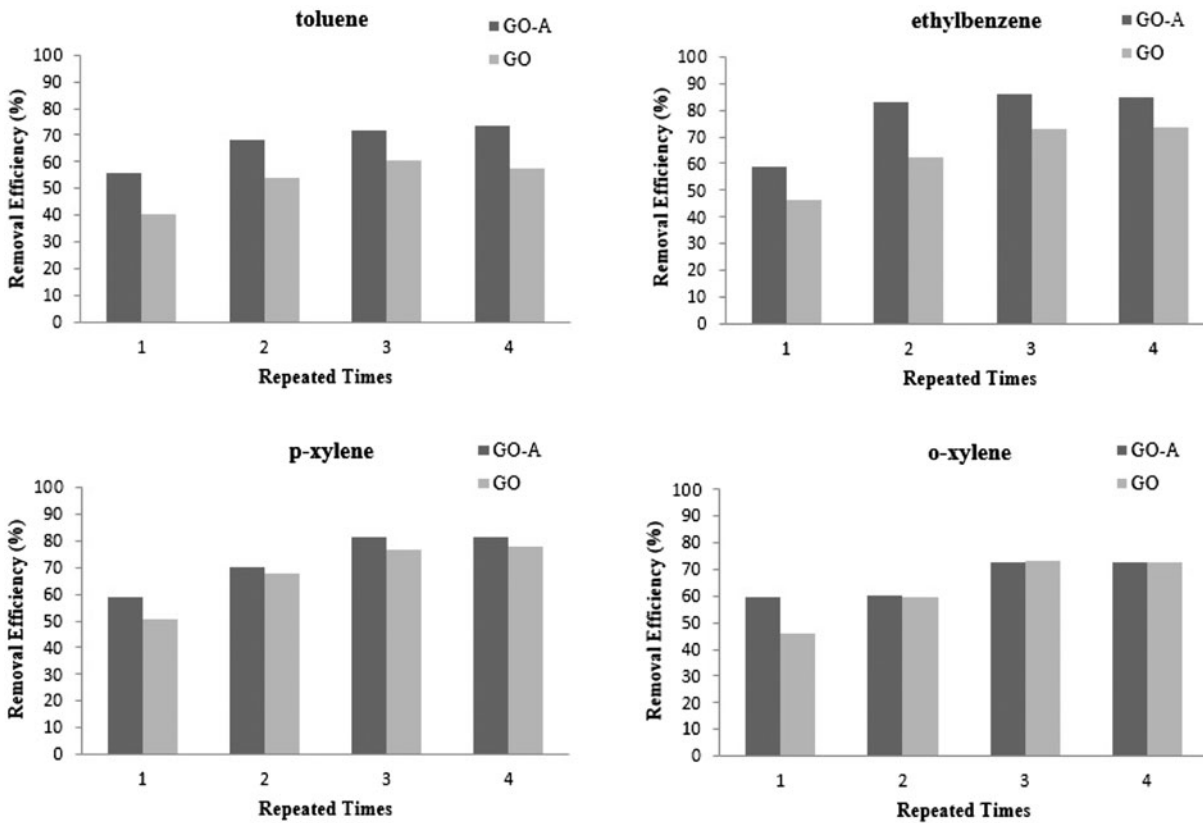


Fig. 11. The regeneration of GO and GO-A (contact time = 5 min; pH 4; initial concentration of TEX = 20 mg/L; adsorbent dose = 1 g/L; agitation speed = 150 rpm; room temperature = 23°C).

Table 7
Comparisons in TEX removal of different adsorbents

Adsorbents	q_e (mg/g)		Conditions				Contact time	Adsorbent dose (g/L)	Refs.
	Toluene	Ethylbenzene	p-Xylene	o-Xylene	Xylenes	C_0 (mg/L)			
Natural zeolite particles with HDTMA-Cl surfactant	0.284	0.232	–	–	0.212	20	48 h	5	[47]
Natural zeolite particles with CPB surfactant	0.381	0.337	–	–	0.320	20	48 h	5	[47]
Granulated zeolite nanoparticles with HDTMA-Cl surfactant	0.898	0.746	–	–	0.674	20	48 h	5	[47]
Granulated zeolite nanoparticles with CPB surfactant	0.954	0.788	–	–	0.724	20	48 h	5	[47]
Carbon nanotube (CNT)	80.1	81.1	147.8	–	–	200	4 h	0.6	[50]
CNT(NaOCl)	252.1	261.2	318.3	–	–	200	4 h	0.6	[50]
CNTs-3.2%O	99.47	115.63	–	–	–	15–110 (toluene)	6 h	0.4	[51]
Activated carbon prepared from date pits	5.0	5.6	–	–	6.2	10	–	1	[52]
Activated carbon prepared from almond shells	5.0	6.5	–	–	7.4	10	–	1	[52]
Activated carbon prepared from olive stones	5.8	6.6	–	–	7.2	10	–	1	[52]
Montmorillonite modified with poly ethylene glycol	4.18	5.12	–	–	6.00	150	24 h	5	[2]
Smectite organoclay	0.69	0.72	0.75	–	–	29.06 (toluene)	60 min	20	[46]
Thermally modified diatomite	0.3	0.6	0.9	0.7	–	–	–	–	[46]
Ostrich bone waste-loaded a cationic surfactant	119.5	144.1	137.7	–	–	100	60 min	10	[53]
GO-A	11.3	13.6	14	12.2	–	20	5 min	1	This work
GO	7.8	9.7	10.2	8.8	–	20	5 min	1	This work

Notes: HDTMA-Cl = hexadecyltrimethylammonium-chloride, CPB = *n*-cetylpyridinium bromide.

4. Conclusions

The aim of this paper was to synthesis the GO and GO modified with 4-aminodiphenylamine. Then this adsorbent was used for the removal of TEX (toluene, ethylbenzene and xylenes) from aqueous solution. The following conclusions can be derived from this study:

- (1) The removal efficiency of toluene, ethylbenzene, p-xylene, and o-xylene at the optimum condition (contact time: 5 min, pH: 4 and adsorbent dose: 1 g/L) was 56, 70, 72, and 66%, respectively.
- (2) The preference of adsorbent in the compounds decreased in the following order: p-xylene → ethylbenzene → o-xylene → toluene.
- (3) The contact time for the adsorption process in the optimum condition was 5 min. It means that this adsorbent has high efficiency for the removal of TEX in the beginning minutes of the process.
- (4) Langmuir isotherm (R^2 in range 0.928–0.981) and pseudo-second-order kinetic (R^2 in range 0.928–0.963) showed good fit to the experimental adsorption data of TEX. Additionally, the error function provided the best parameters for Langmuir isotherm and pseudo-second-order model.
- (5) Based on the results of regeneration study, GO-A can be reused for at least seven cycles for TEX removal. The results are illustrated that GO-A can be suggested as an economic adsorbent.
- (6) The total pore volume and average pore diameter of GO were improved from (0.016 cm³/g, 4.853 nm) to (0.133 cm³/g, 42.879 nm) by modification.
- (7) GO-A is a new adsorbent of carbon family that modified with 4-aminodiphenylamine. These results showed that GO-A is both effective and reproducible adsorbent and it could be used as a promising adsorbent for TEX removal from aqueous solution.

Acknowledgment

We are grateful to the Science and Research Branch, Islamic Azad University (SRBIAU), Iranian Mineral Processing Research Center (IMPRC), and National Iranian Oil Products Distribution Company (NIOOPDC) for providing research materials, equipment and funds. In addition, the authors wish to thank Mrs Armineh Azizi (PhD graduate of Amirkabir

University of Technology (AUT) and Dr Elaheh Kow-sari (Associate Professor of AUT) for their consultations during the experiments as well as Ehssan Hosseini Koupaie (PhD candidate of the University of British Columbia) for kind revise. The authors also appreciate the SRBIAU Laboratory assistants (Ms Elham Dolati and Ms Shima Shakouri).

List of symbols

q_t	—	adsorbent capacity of adsorbate (mg/g)
RE(%)	—	removal efficiency (%)
C_0	—	initial concentration of the adsorbate (mg/L)
C_t	—	concentration of the adsorbate after a certain period of time (mg/L)
m	—	mass of adsorbent (g)
v	—	volume of the solution (L)
q_e	—	adsorption capacity of the adsorbent at equilibrium (mg/g)
C_e	—	concentration of adsorbate at equilibrium (mg/L)
k_1	—	Langmuir constant (l/mg)
Q_m	—	maximum adsorption capacity (mg/g)
k_f	—	Freundlich constant (l/mg)
n	—	a constant related the intensity of adsorption
q_m	—	theoretical monolayer saturation capacity (mg/g)
B	—	constant of the sorption energy (mol ² /kJ ²)
ε	—	Polanyi potential
R	—	universal gas constant (8.314 J/mol K)
T	—	absolute temperature
E	—	the adsorption energy (kJ/mol)
k_1	—	rate constant of pseudo-first-order adsorption (1/min)
k_2	—	rate constant of pseudo-second-order adsorption (g/mg min)
k_p	—	rate constant of the intraparticle diffusion kinetic model (mg/g min ^{1/2})
c	—	a constant in intraparticle diffusion kinetic
a	—	a constant in Elovich model
b	—	a constant in Elovich model
q_{cal}	—	equilibrium capacity estimated from the model (mg/g)
p	—	the number of parameters in the regression model

References

- [1] L. Seifi, A. Torabian, H. Kazemian, G.N. Bidhendi, A.A. Azimi, F. Farhadi, S. Nazmara, Kinetic study of BTEX removal using granulated surfactant-modified natural zeolites nanoparticles, *Water Air Soil Pollut.* 219 (2011) 443–457.
- [2] H. Nourmoradi, M. Nikaen, M. Khiadani (Hajian), Removal of benzene, toluene, ethylbenzene and xylene (BTEX) from aqueous solutions by montmorillonite modified with nonionic surfactant: Equilibrium, kinetic and thermodynamic study, *Chem. Eng. J.* 191 (2012) 341–348.

- [3] M. Aivalioti, I. Vamvasakis, E. Gidarakos, BTEX and MTBE adsorption onto raw and thermally modified diatomite, *J. Hazard. Mater.* 178 (2010) 136–143.
- [4] S.H. Kim, J.H. Park, C.Y. Lee, Surface-functionalized mesoporous silica nanoparticles as sorbents for BTEX, *J. Porous Mater.* 20 (2013) 1087–1093.
- [5] S. Sharmasarkar, W.F. Jaynes, G.F. Vance, BTEX sorption by montmorillonite organo-clays: TMPA, *Water Air Soil Pollut.* 119 (2000) 257–273.
- [6] A.A.M. Daifullah, S.M. Yakout, Adsorption/desorption of BTEX on activated carbon prepared from rice husk, *Desalin. Water Treat.* 52 (2014) 4485–4491.
- [7] F. Simantiraki, E. Gidarakos, Comparative assessment of compost and zeolite utilisation for the simultaneous removal of BTEX, Cd and Zn from the aqueous phase: Batch and continuous flow study, *J. Environ. Manage.* 159 (2015) 218–226.
- [8] Y. He, Y. Liu, T. Wu, J. Ma, X. Wang, Q. Gong, W. Kong, F. Xing, Y. Liu, J. Gao, An environmentally friendly method for the fabrication of reduced graphene oxide foam with a super oil absorption capacity, *J. Hazard. Mater.* 260 (2013) 796–805.
- [9] A. Bhatnagar, F. Kaczala, W. Hogland, M. Marques, C.A. Paraskeva, V.G. Papadakis, M. Sillanpää, Valorization of solid waste products from olive oil industry as potential adsorbents for water pollution control—a review, *Environ. Sci. Pollut. Res.* 21 (2014) 268–298.
- [10] S. Chowdhury, R. Balasubramanian, Recent advances in the use of graphene-family nanoadsorbents for removal of toxic pollutants from wastewater, *Adv. Colloid Interface Sci.* 204 (2014) 35–56.
- [11] J. Song, W. Zou, Y. Bian, F. Su, R. Han, Adsorption characteristics of methylene blue by peanut husk in batch and column modes, *Desalination* 265 (2011) 119–125.
- [12] J.U.K. Oubagaranadin, Z.V.P. Murthy, Isotherm modeling and batch adsorber design for the adsorption of Cu(II) on a clay containing montmorillonite, *Appl. Clay Sci.* 50 (2010) 409–413.
- [13] X. Deng, L. Lü, H. Li, F. Luo, The adsorption properties of Pb(II) and Cd(II) on functionalized graphene prepared by electrolysis method, *J. Hazard. Mater.* 183 (2010) 923–930.
- [14] S. Chowdhury, R. Balasubramanian, Graphene/semiconductor nanocomposites (GSNs) for heterogeneous photocatalytic decolorization of wastewaters contaminated with synthetic dyes: A review, *Appl. Catal. B* 160–161 (2014) 307–324.
- [15] K. Kinoshita, T. Saito, A. Ito, T. Kawakami, Y. Kitagawa, S. Yamanaka, K. Yamaguchi, M. Okumura, Theoretical study on singlet oxygen adsorption onto surface of graphene-like aromatic hydrocarbon molecules, *Polyhedron* 30 (2011) 3249–3255.
- [16] B.T. Zhang, X. Zheng, H.F. Li, J.M. Lin, Application of carbon-based nanomaterials in sample preparation: A review, *Anal. Chim. Acta* 784 (2013) 1–17.
- [17] F. Najafi, Removal of zinc (II) ion by graphene oxide (GO) and functionalized graphene oxide–glycine (GO-G) as adsorbents from aqueous solution: kinetics studies, *Int. Nano Lett.* 5 (2015) 171–178.
- [18] S. Chen, J. Hong, H. Yang, J. Yang, Adsorption of uranium (VI) from aqueous solution using a novel graphene oxide-activated carbon felt composite, *J. Environ. Radioact.* 126 (2013) 253–258.
- [19] F. Li, X. Jiang, J. Zhao, S. Zhang, Graphene oxide: A promising nanomaterial for energy and environmental applications, *Nano Energy* 16 (2015) 488–515.
- [20] L. Xu, X. Yang, Molecular dynamics simulation of adsorption of pyrene–polyethylene glycol onto graphene, *J. Colloid Interface Sci.* 418 (2014) 66–73.
- [21] W. Zou, H. Bai, S. Gao, K. Li, Characterization of modified sawdust, kinetic and equilibrium study about methylene blue adsorption in batch mode, *Korean J. Chem. Eng.* 30(1) (2013) 111–122.
- [22] S. Mitra, P. Roy, BTEX: A serious Ground-water contaminant, *Res. J. Environ. Sci.* 5(5) (2011) 394–398.
- [23] W.S. Hummers, R.E. Offeman, Preparation of graphitic oxide, *J. Am. Chem. Soc.* 80 (1958) 1339.
- [24] A. Heydarinasab, H. Ahmad Panahi, H. Nematzadeh, E. Moniri, S. Nasrollahi, Preparation and characterization of iminodiacetic acid: Magnetite nano-particles as a novel famotidine carrier substrate for sustained drug release, *Monatsh. Chem.* 146 (2015) 411–416.
- [25] N.K. Amin, Removal of direct blue-106 dye from aqueous solution using new activated carbons developed from pomegranate peel: Adsorption equilibrium and kinetics, *J. Hazard. Mater.* 165 (2009) 52–62.
- [26] P. Wu, W. Wu, S. Li, N. Xing, N. Zhu, P. Li, J. Wu, C. Yang, Z. Dang, Removal of Cd²⁺ from aqueous solution by adsorption using Fe-montmorillonite, *J. Hazard. Mater.* 169 (2009) 824–830.
- [27] A. Azizi, M.R. Alavi Moghaddam, M. Arami, Performance of pulp and paper sludge for reactive blue 19 dye removal from aqueous solutions: Isotherm and kinetic study, *J. Residuals Sci. Technol.* 7 (2010) 173–179.
- [28] L. Levankumar, V. Muthukumar, M.B. Gobinath, Batch adsorption and kinetics of chromium (VI) removal from aqueous solutions by *Ocimum americanum* L. seed pods, *J. Hazard. Mater.* 161 (2009) 709–713.
- [29] M. Yuan, S. Tong, S. Zhao, C.Q. Jia, Adsorption of polycyclic aromatic hydrocarbons from water using petroleum coke-derived porous carbon, *J. Hazard. Mater.* 181 (2010) 1115–1120.
- [30] N. Wang, Y. Zhang, F. Zhu, J. Li, S. Liu, P. Na, Adsorption of soluble oil from water to graphene, *Environ. Sci. Pollut. Res.* 21 (2014) 6495–6505.
- [31] V.M. Vučurović, R.N. Razmovski, U.D. Miljić, V.S. Puškaš, Removal of cationic and anionic azo dyes from aqueous solutions by adsorption on maize stem tissue, *J. Taiwan Inst. Chem. Eng.* 45 (2014) 1700–1708.
- [32] A. Azizi, M.R. Alavi Moghaddam, M. Arami, Comparison of three treated pulp and paper sludges as adsorbents for RB19 Dye removal, *J. Residuals Sci. Technol.* 8 (2011) 117–124.
- [33] A.C.A. de Lima, R.F. Nascimento, F.F. de Sousa, J.M. Filho, A.C. Oliveira, Modified coconut shell fibers: A green and economical sorbent for the removal of anions from aqueous solutions, *Chem. Eng. J.* 185–186 (2012) 274–284.
- [34] A. Azizi, M.R. Alavi Moghaddam, M. Arami, Removal of a reactive dye using ash of pulp and paper sludge, *J. Residuals Sci. Technol.* 9 (2012) 159–168.
- [35] P. Sharma, B.K. Saikia, M.R. Das, Removal of methyl green dye molecule from aqueous system using reduced graphene oxide as an efficient adsorbent: Kinetics, isotherm and thermodynamic parameters, *Colloids Surf. A*, 457 (2014) 125–133.

- [36] P. Ganesan, R. Kamaraj, S. Vasudevan, Application of isotherm, kinetic and thermodynamic models for the adsorption of nitrate ions on graphene from aqueous solution, *J. Taiwan Inst. Chem. Eng.* 44 (2013) 808–814.
- [37] K. Zhang, K.C. Kemp, V. Chandra, Homogeneous anchoring of TiO₂ nanoparticles on graphene sheets for waste water treatment, *Mater. Lett.* 81 (2012) 127–130.
- [38] H. Yang, H. Li, J. Zhai, L. Sun, Y. Zhao, H. Yu, Magnetic prussian blue/graphene oxide nanocomposites caged in calcium alginate microbeads for elimination of cesium ions from water and soil, *Chem. Eng. J.* 246 (2014) 10–19.
- [39] V.K. Konaganti, R. Kota, S. Patil, G. Madras, Adsorption of anionic dyes on chitosan grafted poly(alkyl methacrylate)s, *Chem. Eng. J.* 158 (2010) 393–401.
- [40] L.M. Tao, F. Niu, D. Zhang, T.M. Wang, Q.H. Wang, Amorphous covalent triazine frameworks for high performance room temperature ammonia gas sensing, *New J. Chem.* 38 (2014) 2774–2777.
- [41] N.K. Ladani, M.P. Patel, R.G. Patel, A convenient one-pot synthesis of series of 3-(2,6-diphenyl-4-pyridyl)hydroquinolin-2-one under microwave irradiation and their antimicrobial activities, *Indian J. Chem.* 48B (2009) 261–266.
- [42] S.M. Yuen, C.C.M. Ma, Y.Y. Lin, H.C. Kuan, Preparation, morphology and properties of acid and amine modified multiwalled carbon nanotube/polyimide composite, *Compos. Sci. Technol.* 67 (2007) 2564–2573.
- [43] C. Wang, J. Zhou, J. Ni, Y. Cheng, H. Li, Design and synthesis of pyrophosphate acid/graphene composites with wide stacked pores for methylene blue removal, *Chem. Eng. J.* 253 (2014) 130–137.
- [44] J. Li, Y. Yu, S.J. Bao, Q.Q. Sun, Experimental investigation of the important influence of pretreatment process of thermally exfoliated graphene on their microstructure and supercapacitor performance, *Electrochim. Acta* 180 (2015) 187–195.
- [45] S. Sheshmani, A. Ashori, S. Hasanzadeh, Removal of Acid Orange 7 from aqueous solution using magnetic graphene/chitosan: A promising nano-adsorbent, *Int. J. Biol. Macromol.* 68 (2014) 218–224.
- [46] M.N. Carvalho, M.D. da Motta, M. Benachour, D.C.S. Sales, C.A.M. Abreu, Evaluation of BTEX and phenol removal from aqueous solution by multi-solute adsorption onto smectite organoclay, *J. Hazard. Mater.* 239–240 (2012) 95–101.
- [47] L. Seifi, A. Torabian, H. Kazemian, G.N. Bidhendi, A.A. Azimi, A. Charkhi, Adsorption of petroleum monoaromatics from aqueous solutions using granulated surface modified natural nanozeolites: Systematic study of equilibrium isotherms, *Water Air Soil Pollut.* 217 (2011) 611–625.
- [48] L. Wang, J. Zhang, R. Zhao, C. Li, Y. Li, C. Zhang, Adsorption of basic dyes on activated carbon prepared from *Polygonum orientale* Linn: Equilibrium, kinetic and thermodynamic studies, *Desalination* 254 (2010) 68–74.
- [49] Y. Li, Y. Sun, F. Dong, W.K. Ho, Enhancing the photocatalytic activity of bulk g-C₃N₄ by introducing mesoporous structure and hybridizing with graphene, *J. Colloid Interface Sci.* 436 (2014) 29–36.
- [50] C. Lu, F. Su, S. Hu, Surface modification of carbon nanotubes for enhancing BTEX adsorption from aqueous solutions, *Appl. Surf. Sci.* 254 (2008) 7035–7041.
- [51] F. Yu, J. Ma, Y. Wu, Adsorption of toluene, ethylbenzene and m-xylene on multi-walled carbon nanotubes with different oxygen contents from aqueous solutions, *J. Hazard. Mater.* 192 (2011) 1370–1379.
- [52] A.A.M. Daifullah, B.S. Girgis, Impact of surface characteristics of activated carbon on adsorption of BTEX, *Colloids Surf. A*, 214 (2003) 181–193.
- [53] H. Shakeri, M. Arshadi, J.W.L. Salvacion, Removal of BTEX by using a surfactant—Bio originated composite, *J. Colloid Interface Sci.* 466 (2016) 186–197.